Journal of Pharmaceutical Analysis 15 (2025) 101079

Contents lists available at ScienceDirect

Journal of Pharmaceutical Analysis

journal homepage: www.elsevier.com/locate/jpa

Short communication

Distribution of pamiparib, a novel inhibitor of poly(ADP-ribose)-polymerase (PARP), in tumor tissue analyzed by multimodal imaging

Lavinia Morosi [a, *], Sara Timo [a], Rosy Amodeo [a, b], Monica Lupi [a], Marina Meroni [c], Ezia Bello [c], Roberta Frapolli [c], Giuseppe Martano [a, d], Maurizio D'Incalci [a, b]

[a] IRCCS Humanitas Research Hospital, Rozzano, 20089, Italy
[b] Department of Biomedical Sciences, Humanitas University, Pieve Emanuele, 20072, Italy
[c] Istituto di Ricerche Farmacologiche Mario Negri IRCCS, Department of Oncology, Milan, 20253, Italy
[d] Institute of Neuroscience, National Research Council of Italy (CNR) c/o Humanitas Mirasole S.p.A, Rozzano, 20089, Italy

ARTICLE INFO

Article history:
Received 29 May 2024
Received in revised form
31 July 2024
Accepted 21 August 2024
Available online 24 August 2024

Pamiparib is a potent and selective oral poly(adenosine diphosphate (ADP)-ribose)-polymerase (PARP)1/2 inhibitor (PARPi). Pamiparib has good bioavailability and shows greater cytotoxic potency and similar DNA-trapping capacity compared to olaparib. It is not affected by adenosine triphosphate (ATP)-binding cassette transporters. Consequently, pamiparib may be useful in overcoming drug resistance caused by poor drug distribution in tumor due to overexpression of this efflux pump [1]. Mass spectrometry imaging (MSI) is a powerful technology that allows to study drugs distribution in tissues while maintaining spatial information [2]. Here, MSI was applied to visualize pamiparib in tumor in combination with spatial metabolomics and lipidomics, liquid chromatography-tandem mass spectrometry (LC-MS/MS) analysis, immunofluorescence analysis, and histological staining to gain a comprehensive understanding of how pamiparib is distributed. The results show that pamiparib was evenly distributed in ovarian tumor models, including those that overexpress P-glycoprotein (P-gp). In contrast, olaparib was not detected by MSI in any of the analyzed tumors, despite the comparable sensitivity of the analytical method. This difference in tumor distribution was confirmed by LC-MS/MS analysis.

A factor leading to chemoresistance is the limited distribution of drugs within tumor tissue, due to the heterogeneity of the tumor microenvironment. We previously reported that the distribution of drug within tumor tissue is heterogeneous among different tumor models. Drug penetration was limited and irregular in solid tumors with necrotic or fibrotic areas and irregular blood vessels [3].

MSI method was developed to visualize pamiparib and olaparib using α-cyano-4-hydroxycinnamic (HCCA) as matrix (Figs. S1 and S2). The linearity and limit of detection were assessed as reported in Fig. S3. The method was applied to study the distribution of pamiparib in the ovarian cancer model wild type (WT) (A2780 WT) or overexpressing P-gp (A2780P-gp) with 100 μm pixel size. The A2780P-gp model was obtained by our group by repeated exposures to drug and characterized for drug sensitivity, cell cycle perturbations, DNA damage, and DNA repair protein expression. Procedures involving animals and their care were conducted in accordance with the national and international laws, regulations, and policies governing the care and use of laboratory animals (ethical approval number: 475/2017-PR; details are shown in Supplementary data).

MSI images normalized over deuterated pamiparib ion signal show that pamiparib is homogeneously distributed in tumor tissue without difference between WT and P-gp-overexpressing tumors, thus directly demonstrating that pamiparib is not a substrate of P-gp (Figs. 1A and S4). In contrast, olaparib was undetectable in tumors by MSI (Fig. S5). Notably, the sensitivity of the analytical method was comparable for the two drugs (Fig. S3). An adjacent section was analyzed by hematoxylin and eosin (H&E) staining, and no macroscopic difference in tissue morphology can be pointed out comparing A2780 WT and A2780P-gp. The fine laser diameter of the ion source allowed us to obtain images of pamiparib distribution at a 10 μm pixel size to create a more detailed picture of the drug penetration in tissue (Fig. 1A). This allowed most informative comparison of MSI data with immunofluorescence images, which are characterized by superior spatial resolution, in order to correlate drug distribution with P-gp presence. This analysis confirmed the P-gp overexpression in A2780P-gp tumors compared to A2780 WT and highlighted the homogeneity of pamiparib distribution independently by the presence of this efflux pump. The MSI data generated have sufficient spatial resolution to potentially

* Corresponding author.
E-mail address: lavinia.morosi@humanitasreserach.it (L. Morosi).
Peer review under responsibility of Xi'an Jiaotong University.

https://doi.org/10.1016/j.jpha.2024.101079

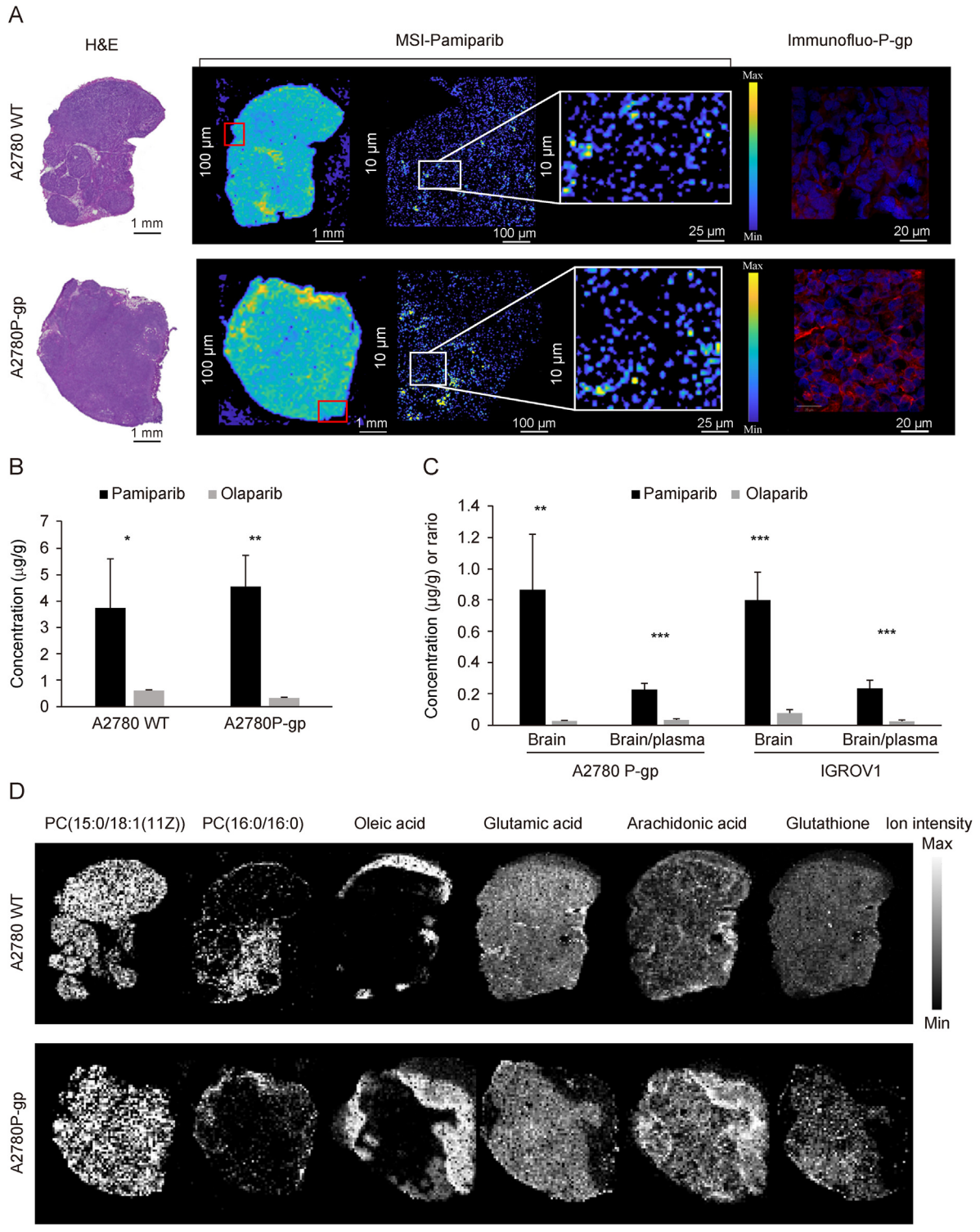

Fig. 1. Influence of P-gp overexpression on pamiparib tissue distribution. (A) Pamiparib distribution by mass spectrometry imaging (MSI) in a representative section of the ovarian cancer model wild type (WT) (A2780 WT) or overexpressing P-glycoprotein (P-gp) (A2780P-gp) with hematoxylin and eosin (H&E) staining of the adjacent section. The red square on the sequential section was acquired at a 10 µm pixel size. The enlargement of the white square was shown in the right panel to allow the comparison with immunofluorescence analysis (red,> P-gp; blue, 4′,6-diamidino-2-phenylindole (DAPI)). (B) Quantitative determination of pamiparib and olaparib in tumor tissue by liquid chromatography-tandem mass spectrometry (LC-MS/MS) in A2780 WT and A2780P-gp. (C) Brain concentrations and brain/plasma ratios of the drug concentration for pamiparib and olaparib in both tumor models. $^{*}P < 0.05$, $^{**}P < 0.01$, $^{***}P < 0.001$ ($n = 3$). (D) Distribution of selected metabolites and lipids identified on serial sections was compared to that used for pamiparib distribution.

allow the determination of drug distribution at the cellular level (10 µm), discriminating different cellular populations and tumor microenvironment sub compartments after accurate image co-registration and performing the analysis on the same slice.

The difference in tumor distribution of pamiparib and olaparib was confirmed by LC-MS/MS analysis, gold standard for pharmacokinetics analysis (Tables S1–S6). Total pamiparib and olaparib concentrations in tumor tissue highlight a significant difference in

drug penetration between the two drugs in both tumor models (Fig. 1B). No difference could be detected in pamiparib concentrations comparing A2780 WT and A2780P-gp tumors. Results were confirmed in another ovarian cancer model: IGROV1 parental and P-gp overexpressing (Fig. S6).

Since P-gp is involved in blood-brain-barrier functions, the brain penetration of pamiparib might be higher than that of olaparib. Fig. 1C shows that pamiparib reached significantly higher concentrations in brain tissue of treated mice than olaparib with favorable brain/plasma ratio suggesting that pamiparib can be proposed to treat brain tumors.

Moreover, pamiparib can be proposed after olaparib treatment in case of acquired resistance against the drug. The major mechanism of resistance against PARPi is the reactivation of homologous recombination function, but also other mechanisms such as overexpression of P-gp have been reported [4]. Therefore, pamiparib could be advantageous, as its tumor distribution is unaffected by the expression of P-gp.

Finally, spatial metabolomics analysis was performed untargeted on serial sections using HCCA and 1,5-diaminonaphthalene (DAN) as matrix and analyzing positive and negative ions, respectively. A total of 591 compounds were annotated comprising amino acids, nucleotides, and lipids using an in house developed pipeline [5]. The complete list of annotated metabolites is shown in Tables S7 and S8. Figs. 1D, S7 and S8 show the distribution of representative metabolites and lipids in tumors supporting the extreme metabolic heterogeneity of tumor tissue. However, the distribution of pamiparib does not appear to be influenced by this heterogeneity.

This approach offers a unique perspective on the intricate relationship between tissue microenvironment, metabolic reprogramming and the pharmacokinetic/pharmacodynamics properties of drugs. In fact, the analysis of various local factors at play, lack of oxygen and nutrients, ATP/ADP ratio and high levels of lactate, alongside the drug distribution, gives a more comprehensive understanding of both resistance and effectiveness mechanisms. Of particular interest in our pipeline is the ability to track the presence of free fatty acids, main mediator of cell proliferation and involved in the modulation of immune responses; arginine and proline whose metabolism is altered in many solid tumors and glutathione, which is linked to hypoxia that contributes to tumor progression and drug resistance.

One limitation of our study is that the animal model was chosen to investigate the effect of P-gp overexpression on pamiparib tumor distribution and pharmacokinetics, but it is not homologous recombination (HR) deficient and consequently it is not overly sensitive to PARPi. Thus, this model was not ideal for correlating how PARPi concentration correlates with antitumor effect. Nevertheless, the results show the eminent feasibility of integrating spatial pharmacokinetic and pharmacodynamic effects with potential applications at the clinical level to elucidate mechanisms of sensitivity to, and resistance against, PARPi as well as other anticancer drugs.

In conclusion, pamiparib tumor distribution was optimal and not affected by P-gp overexpression and tumor metabolic heterogeneity. Pamiparib showed overall better tumor penetration than olaparib as shown by MSI and LC-MS/MS. The multimodal method developed to visualize pamiparib in tissues in correlation with histological staining, immunofluorescence and spatial metabolomics shows high sensitivity and specificity suggesting the possibility to apply MSI in a clinical setting to understand the correlation between tumor drug distribution, chemoresistance and antitumor efficacy in a more comprehensive way.

CRediT authorship contribution statement

Lavinia Morosi: Writing – original draft, Visualization, Methodology, Investigation, Conceptualization. **Sara Timo:** Validation, Methodology. **Rosy Amodeo:** Validation, Methodology. **Monica Lupi:** Visualization, Investigation. **Marina Meroni:** Methodology, Investigation. **Ezia Bello:** Methodology, Investigation. **Roberta Frapolli:** Supervision, Resources, Conceptualization. **Giuseppe Martano:** Writing – review & editing, Software, Data curation. **Maurizio D'Incalci:** Writing – review & editing, Supervision, Funding acquisition, Conceptualization.

Declaration of competing interest

The authors declare that there are no conflicts of interest.

Acknowledgments

The study was supported in part by funding from BeiGene, Ltd., USA (Grant No.: KPR081) with additional support from the Alessandra Bono Foundation, Italy. The authors acknowledge Prof. Andreas Gescher for its critical revision and editing of the article. The authors acknowledge the Metabolomics and Pharmacokinetics unit at IRCCS Humanitas Research Hospital, Italy, for technical support.

Appendix A. Supplementary data

Supplementary data to this article can be found online at https://doi.org/10.1016/j.jpha.2024.101079.

References

[1] Y. Xiong, Y. Guo, Y. Liu, et al., Pamiparib is a potent and selective PARP inhibitor with unique potential for the treatment of brain tumor, Neoplasia 22 (2020) 431–440.
[2] Y. Chen, Y. Liu, X. Li, et al., Recent advances in mass spectrometry-based spatially resolved molecular imaging of drug disposition and metabolomics, Drug Metab. Dispos. 51 (2023) 1273–1283.
[3] L. Morosi, C. Matteo, T. Ceruti, et al., Quantitative determination of niraparib and olaparib tumor distribution by mass spectrometry imaging, Int. J. Biol. Sci. 16 (2020) 1363–1375.
[4] A. Vaidyanathan, L. Sawers, A.L. Gannon, et al., ABCB1 (MDR1) induction defines a common resistance mechanism in paclitaxel- and olaparib-resistant ovarian cancer cells, Br. J. Cancer 115 (2016) 431–441.
[5] L. Morosi, M. Miotto, S. Timo, et al., A fully automated pipeline for compound annotation and quantitation in mass spectrometry imaging experiments, Brief. Bioinform. 25 (2023), bbad463.